*Tellus* (1989), *41A*, 246–254

# Idealized model for stratocumulus cloud layer thickness

By ALAN K. BETTS, *RD2, Box 3300, Middlebury, VT 05753, USA*

(Manuscript received 22 March 1988; in final form 18 July 1988)

ABSTRACT

Equilibrium solutions are constructed using an idealized model for mixed and partially mixed boundary layers to show the dependence of the equilibrium cloud layer thickness on different physical processes. The condition when a mixed layer becomes cloud-free is reduced to a comparison between three pressure scales, associated with the surface wind and divergence, the radiative cooling and the subsaturation of the entrained air. The evaporation of layer cloud by cloud-top mixing is also formulated in terms of simple pressure scales.

## 1. Introduction

This paper discusses the solutions for cloud-layer thickness of an idealized convective boundary layer (CBL) model (Betts, 1983). Cloud layer thickness is related to three contributing factors: the surface forcing, the radiative forcing and the cloud top entrainment of dry air. The magnitude of each of these processes will be expressed in terms of pressure scales, whose sum determines cloud layer thickness. The prediction of cloud layer thickness and fractional cloudiness remains a difficult task in global forecast and climate models, and the observational study of clouds and their radiative effects is the major objective of the International Satellite Cloud Climatology Project (ISCCP). In this paper, horizontal homogeneity will be assumed, so that the model solutions are a more realistic representation of stratocumulus than broken cloud fields. In addition, in this idealized analysis, boundary layer depth and the mean radiative cooling (or heating) rate in the convective boundary layer are specified parameters.

Mixed-layer models for the cloudy boundary layer have a long history (Lilly, 1968; Schubert, 1976; Schubert et al., 1979a, b; Stage and Businger, 1981a, b; Fitzjarrald, 1982). Betts (1983) used conserved variable diagrams to show the balance of surface, entrainment, and radiative fluxes. This paper extends this work to include a partially mixed cloudy boundary layer and to develop an approximate analytic framework for understanding mean-layer cloud thickness in cloudy boundary layers. Other simple models for partially mixed boundary layers have been largely developed for modelling shallow cumulus boundary layers (Betts, 1973, 1975, 1976; Sarachik, 1974; Ogura and Cho, 1974; Albrecht et al., 1979, Albrecht, 1979, 1981; Augstein and Wendel, 1980). Betts (1986) suggested that the thermodynamic structure of CBLs could be represented in general by mixing line models. This approach will be taken here.

## 2. Budget equation for idealized structure

Fig. 1 shows the thermodynamic structure for an idealized partially mixed boundary layer. The diagram is a $\theta^*$, $q^*$ plot, where the conserved variables are saturation point (SP) potential temperature and mixing ratio. For unsaturated air these are the familiar $\theta$, and $q$ and the parcel SP is the thermodynamic point of the lifting condensation level; while for cloudy air they are liquid water potential temperature and total water. On this plot, the isobars or saturation pressure lines ($p^*$) are curved while the moist adiabats ($\theta_{ES} = 340$ K is shown dashed on Fig. 1) are nearly linear. $\underset{\sim}{M}$ is the layer mean SP, $\underset{\sim}{Q}$ the SP of the surface, $\underset{\sim}{T}$ the SP of air above the boundary layer which is being entrained into it. The layer has a gradient of thermodynamic properties

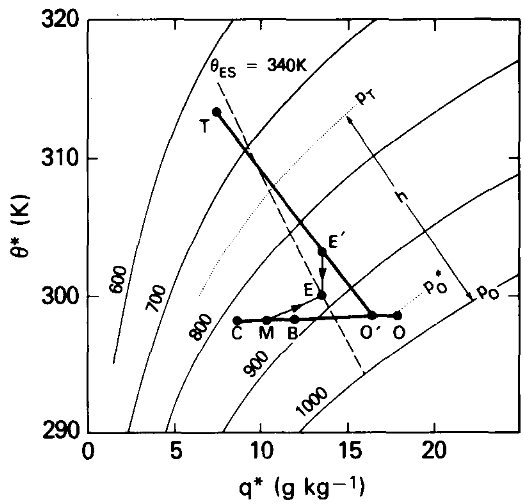


*Fig. 1.* Saturation point diagram for non-equilibrium, partially mixed CBL with radiative cooling.

$\underset{\sim}{S}$ with height from $\underset{\sim}{B}$ to $\underset{\sim}{C}$, which we shall suppose is a uniform change with pressure along a mixing line (Betts, 1982). Mixing lines are straight lines on this diagram. We have drawn the mixing line $\underset{\sim}{O}\underset{\sim}{B}\underset{\sim}{C}$ slightly unstable to the dry adiabat (constant $\theta^*$). This is typical of stratocumulus off the south-western coast of California with advection over warmer water associated with a northerly low level flow. At the boundary layer top ($p_T$), we shall assume a sharp thermodynamic transition from $\underset{\sim}{C}$ to $\underset{\sim}{T}$. $\underset{\sim}{O}'$, $\underset{\sim}{E}'$ and $\underset{\sim}{E}$ are defined later.

Consider a horizontally homogeneous time-dependent layer of instantaneous (pressure) thickness, $h = p_0 - p_T$. Following Betts (1983), the vertically integrated thermodynamic budget equation for the layer with vertical SP profile, $\underset{\sim}{S}$, and mean, $\underset{\sim}{M}$, can be written

$$h\dot{\underset{\sim}{M}} = \omega_0(\underset{\sim}{O} - \underset{\sim}{B}) - \int_{p_T}^{p_0} (\omega(p)\,\partial \underset{\sim}{S}/\partial p)\,\mathrm{d}p + \dot{h}(\underset{\sim}{T} - \underset{\sim}{M}) + h\dot{\theta}_R, \tag{1}$$

where the overdot denotes a time derivative, $\omega(p)$ is the mean vertical motion (which we shall suppose is subsiding), $\omega_0$ (defined positive) is a surface transfer coefficient ($\rho g C_D V_0$, where $C_D$ is a drag coefficient, and $V_0$ the surface wind speed), and $\dot{\theta}_R$ is the mean radiative heating (or cooling) rate for the whole CBL. We shall simplify (1) by considering constant divergence, $D$, so that

$$\omega(p) = D(p_0 - p) \tag{2a}$$

and at the CBL top

$$\omega_h = Dh. \tag{2b}$$

Then (1) simplifies for all profiles of $\underset{\sim}{S}$ to

$$h\dot{\underset{\sim}{M}} = \omega_0(\underset{\sim}{O} - \underset{\sim}{B}) + (Dh + \dot{h})(\underset{\sim}{T} - \underset{\sim}{M}) + h\dot{\theta}_R. \tag{3}$$

This relates the time dependence of the mixed-layer mean to the surface fluxes, the entrainment at the top of the CBL and the mean radiative heating rate. This entrainment term is not the entrainment flux one might measure by aircraft at the base of the inversion: this would be $(Dh + \dot{h})(\underset{\sim}{T} - \underset{\sim}{C})$. However the mean budget equations (1) and (3) consider the impact of entrainment of air with properties $T$ on the layer *average* $\underset{\sim}{M}$ (see Deardorff, 1974; Betts, 1974b). We shall consider equilibrium solutions of (3).

## 3. Equilibrium solutions

### *3.1. Equilibrium state*

We shall replace $\underset{\sim}{B}$ in (3) by defining a modified surface SP

$$\underset{\sim}{O}' = \underset{\sim}{O} + (\underset{\sim}{M} - \underset{\sim}{B}). \tag{4}$$

For a mixed layer $\underset{\sim}{B} = \underset{\sim}{M}$ and $\underset{\sim}{O}' = \underset{\sim}{O}$, but, for a partially mixed layer, $\underset{\sim}{O}'$ is shifted from $\underset{\sim}{O}$ up the mixing line of the CBL (see Fig. 1).

We can also define an equilibrium state $\underset{\sim}{E}$, which satisfies

$$0 = \omega_0(\underset{\sim}{O}' - \underset{\sim}{E}) + (Dh + \dot{h})(\underset{\sim}{T} - \underset{\sim}{E}) + h\dot{\theta}_R. \tag{5}$$

This represents the balance of surface, entrainment and radiative fluxes. By substituting (4) in (3) and subtracting (5) we obtain

$$\dot{\underset{\sim}{M}} = (\underset{\sim}{E} - \underset{\sim}{M})(\omega_0 + \omega_e)/h = (\underset{\sim}{E} - \underset{\sim}{M})/\tau, \tag{6}$$

where

$$\omega_e = Dh + \dot{h} \tag{7}$$

is the entrainment velocity at boundary layer top. This describes the approach of $\underset{\sim}{M}$ towards an equilibrium state $\underset{\sim}{E}$ which satisfies from (6)

$$\underset{\sim}{E} = (\omega_0 \underset{\sim}{O}' + \omega_e \underset{\sim}{T})/(\omega_0 + \omega_e) + \dot{\theta}_R \tau, \tag{8}$$

with a mean-layer adjustment timescale

$$\tau = h/(\omega_0 + \omega_e). \tag{9}$$

This equilibrium solution $\underset{\sim}{E}$ is the weighted average of $\underset{\sim}{Q}'$, $\underset{\sim}{T}$; modified (at constant $q$) by radiation. The transformation from $\underset{\sim}{Q}$ to $\underset{\sim}{Q}'$ has enabled us to construct a mixed layer model, as in Betts (1983), for a turbulently coupled, but not well-mixed layer. In Fig. 1, $\underset{\sim}{E}'$ lies on the mixing line between $\underset{\sim}{Q}'$ and $\underset{\sim}{T}$ and is given by

$$\underset{\sim}{E}' = (\omega_0 \underset{\sim}{Q}' + \omega_e \underset{\sim}{T})/(\omega_0 + \omega_e). \tag{8'}$$

The radiative term shifts the equilibrium state from $\underset{\sim}{E}'$ to $\underset{\sim}{E}$.

In equilibrium, $\underset{\sim}{M} \to \underset{\sim}{E}$ and $\dot{\underset{\sim}{M}} = \dot{h} = 0$, and the entrainment velocity, $\omega_e = \omega_h = Dh$: the mean subsidence at the equilibrium CBL top height $h$. The timescale $\tau$ in (9) can be expressed in terms of the mean divergence and a surface transfer timescale $\omega_0/h$

$$1/\tau = (D + \omega_0/h). \tag{10}$$

This mean layer adjustment timescale can be large (Schubert, 1976), typically of order a day (see Table 1).

The radiative heating or cooling rate in (5) can be re-expressed in terms of a radiative change of saturation level (SL), $\omega_R^*$:

$$h\dot{\theta}_R = h\omega_R^*(\partial\theta/\partial p)_{qs} = \omega_R^* \Delta\theta_R, \tag{11}$$

where we have further defined for convenience a parameter $\Delta\theta_R$ which is (to the extent that $(\partial\theta/\partial p)_{qs}$ may be taken as constant in the CBL) just the potential temperature difference across the CBL along the $q$ isopleth through $\underset{\sim}{M}$. $\omega_R^*$ is the rate of change of the layer mean SL due to radiative processes: for example the rate at which radiative cooling will thicken a cloud layer with a fixed top. Substituting (9) and (11) in (8) gives

$$\underset{\sim}{E} = (\omega_0 \underset{\sim}{Q} + \omega_e \underset{\sim}{T} + \omega_R^* \Delta\theta_R)/(\omega_0 + \omega_e). \tag{12}$$

Table 1 gives 3 sets of values. The first line represents a shallow CBL (120 mb depth) with moderately high subsidence and divergence typical of stratocumulus in subsidence regimes, and the second is representative of the weaker divergence over much of the tropical oceans, where the CBL and the subsidence are in near balance with the background radiative cooling and radiatively driven subsidence (Betts and Albrecht, 1987; Betts and Ridgway, 1988). The third example with the strongest subsidence and divergence will be discussed later: it will just satisfy a no-cloud condition. $\omega_0$ corresponds to a surface wind speed of 7.8 m s$^{-1}$ and an oceanic bulk transfer coefficient, $C_D$, of $1.3 \cdot 10^{-3}$. Over much of the oceans, the timescale $\tau$ is of order a day. The values of $\omega_R^*$ of 40 and 25 mb day$^{-1}$ correspond to mean cooling rates of 3 and 1.75 K day$^{-1}$ respectively. The right hand part of Table 1 is discussed below.

### 3.2. *Equilibrium cloud layer thickness*

These horizontally homogeneous SP models give particularly simple solutions for cloud thickness. They indicate the relative importance of different physical processes and also illustrate the reduction in cloud thickness from mixed to partially mixed boundary layers. Eqs. (8) and (12) give saturation potential temperature and mixing ratio ($\theta^*$ and $q^*$) for the equilibrium solution. $\theta^*$ and $q^*$ (which are liquid water potential temperature and total water mixing ratio within cloud) are the extensively conserved parameters in a mixing process: while radiative cooling only changes $\theta^*$. To a fair approximation, satisfactory for a qualitative analysis (see Appendix), we can consider saturation level pressure $p^*$ as a variable conserved in mixing by expressing it as a linearized combination of $\theta^*$ and $q^*$ (Betts, 1983). This gives approximate, but very useful illustrative solutions for the CBL cloud thickness. Conceptually, the $p^*$ budget is important because it describes the tendency of a layer towards

Table 1. *Boundary layer parameters*

| $\omega_0$ (mb day$^{-1}$) | $h$ (mb) | $\omega_e$ (mb day$^{-1}$) | $D$ (s$^{-1}$) | $\tau$ (days) | $\omega_R^*$ (mb day$^{-1}$) | $\mathscr{P}_T$ (mb) | $\pi_0$ (mb) | $\pi_R$ (mb) | $h_c$ $\beta = 0$ (mb) | $\beta_c$ |
|---|---|---|---|---|---|---|---|---|---|---|
| 100 | 120 | 60 | $5 \cdot 10^{-6}$ | 0.75 | 40 | −150 | 200 | 80 | 49 | 0.33 |
| 100 | 200 | 40 | $2 \cdot 10^{-6}$ | 1.43 | 25 | −150 | 500 | 125 | 136 | 0.58 |
| 100 | 100 | 65 | $6.5 \cdot 10^{-6}$ | 0.61 | 30 | −200 | 154 | 46 | 0 | |

saturation. At saturation, clouds appear, and these have a major radiative impact. So we may regard the $p^*$ budget as a crucial link between the thermodynamic and radiative budgets.

*3.2.1. Well mixed layer.* For a well-mixed layer, the saturation level $p_E^*$ of $\underset{\sim}{E}$ in (12) will also be the mean cloud base. Treating $p^*$ as an approximately conserved parameter (see Appendix), $p_E^*$ is a weighted average of the SL pressures $p_0^*$, $p_T^*$ of the surface air, and the air entrained at cloud-top, modified by radiation

$$p_E^* = (\omega_0 p_0^* + \omega_e p_T^* + \omega_R^* h)/(\omega_0 + \omega_e). \tag{13}$$

Subtracting $p_E^*$ from the boundary layer top pressure $p_T = p_0 - h$ gives the mean cloud layer thickness

$$\begin{aligned} h_c &= \{(h + \mathscr{P}_0)\,\omega_0 + \omega_e \mathscr{P}_T + h\omega_R^*)/(\omega_0 + \omega_e)\} \\ &= \tau\{\omega_0(1 + \mathscr{P}_0/h) + \omega_e(\mathscr{P}_T/h) + \omega_R^*\}, \end{aligned} \tag{14}$$

where $\mathscr{P}_0$, $\mathscr{P}_T$ are the saturation pressure departures, $(p^* - p)$, for the surface and entrained air respectively.

This equation shows the balance of the different processes in determining cloud layer thickness. There are three $\omega$-velocities associated with the surface wind, the entrainment rate and the radiative process. Two of these ($\omega_0$, and $\omega_e$) control $\tau$ through (9). There are two parameters $\mathscr{P}_0$, $\mathscr{P}_T$ related to the subsaturation of the air at the surface and the air entrained through the inversion.

Over the ocean $\mathscr{P}_0 = 0$ (air is saturated at the ocean surface pressure) so that the cloud thickness is given by

$$h_c = \tau\{\omega_0 + \omega_e(\mathscr{P}_T/h) + \omega_R^*\}. \tag{15}$$

The surface and radiative processes increase cloud thickness and the entrainment of unsaturated air reduces it ($\mathscr{P}_T$ is negative). The criterion for no layer cloud is clearly of interest. It is

$$(\omega_0 + \omega_R^*) < \omega_e|\mathscr{P}_T|/h. \tag{16}$$

The first two sets of values shown in Table 1 give cloud for boundary layers that are well mixed. Stronger subsidence ($\omega_e$) and larger negative $\mathscr{P}_T$ for the entrained air are needed to satisfy (16).

*3.2.2. Pressure scale formulation.* One manipulation of (14) is of conceptual interest. If we substitute from (7) (for an equilibrium layer with $\dot{h} = 0$) in (15), we get

$$\begin{aligned} h_c &= h(\omega_0 + D\mathscr{P}_T + \omega_R^*)/(\omega_0 + Dh) \\ &= h(\pi_0 + \pi_R + \mathscr{P}_T)/(\pi_0 + h), \end{aligned} \tag{17}$$

where two pressure scales have been defined

$$\pi_0 = \omega_0/D, \pi_R = \omega_R^*/D. \tag{18}$$

Schubert (1976), Schubert et al. (1979a, b) and Fitzjarrald (1982) noted the importance of the pressure scale $\pi_0$ for boundary layer equilibrium. The criteria (16) for no cloud has now been reduced to the comparison of pressure scales

$$\pi_0 + \pi_R \leqslant |\mathscr{P}_T|. \tag{19}$$

Table 1 shows values for $\pi_0$ and $\pi_R$. $\pi_0$, the pressure scale associated with the surface fluxes, is typically large compared with the subsaturation $\mathscr{P}_T$, so that it is hard to achieve the no cloud criteria (19) over the oceans. The first two lines in Table 1 do not indeed satisfy (19), and the second to last column gives the corresponding cloud thickness for a well mixed layer. The third example has stronger divergence ($6.5 \times 10^{-6}$ s$^{-1}$) and more unsaturated entrained air ($\mathscr{P}_T = -200$ mb) and just satisfies (19) giving zero cloud thickness.

*3.2.3. Partially mixed boundary layer.* If the boundary layer is only partially mixed, then (13) becomes

$$p_E^* = (\omega_0 p_{0'}^* + \omega_e p_T + h\omega_R^*)/(\omega_0 + \omega_e). \tag{20}$$

The shift from $\underset{\sim}{Q}$ to $\underset{\sim}{Q}'$ in (20) lifts the saturation level of the layer mean. However, in general, $p_E^*$ is no longer the level of cloud-base. Within the boundary layer, the SL, $p^*$, is now a function of pressure and we shall use the simple parameterization suggested by Betts (1986)

$$\beta = \mathrm{d}p^*/\mathrm{d}p \tag{21}$$

and assume $\beta$ is a constant for the CBL. $\beta = 0$ corresponds to a well mixed layer, and $\beta > 0$ to a layer which is thermodynamically coupled, but not well-mixed. A boundary layer capped by clouds also requires $\beta < 1$. Hence

$$p^*(p) = p_E^* + \beta(p - p_0 + \tfrac{1}{2}h). \tag{22}$$

Cloud base $p_c^*$ is at the level where $p_c = p_c^*$, giving

$$p_c^* = (p_E^* - (p_0 - \tfrac{1}{2}h))/(1 - \beta). \tag{23}$$

The corresponding cloud thickness is

$$h_c = \tau\{\omega_0(1 + \mathscr{P}_0/h - \beta) + \omega_e(\mathscr{P}_T/h - \tfrac{1}{2}\beta) + \omega_R^*\}/(1 - \beta). \quad (24)$$

Over the oceans, $\mathscr{P}_0 = 0$, and we get a cloud thickness

$$h_c = \tau\{\omega_0 + (\omega_e(\mathscr{P}_T/h - \tfrac{1}{2}\beta) + \omega_R^*)/(1 - \beta)\} \quad (25a)$$

$$= h\{\pi_0 + [\mathscr{P}_T - \tfrac{1}{2}\beta h + \pi_R]/(1 - \beta)\}/(\pi_0 + h), \quad (25b)$$

if we substitute the pressure scales $\pi_0$, and $\pi_R$ from (18). Generally the cloud thickness for a partially mixed layer is reduced, and for some value of say $\beta_c$, the stratiform cloud layer vanishes. From (25a) $\beta_c$ is given by

$$\beta_c = (\omega_0 + \omega_e(\mathscr{P}_T/h) + \omega_R^*)/(\omega_0 + \tfrac{1}{2}\omega_e). \quad (26)$$

If we substitute from (14), supposing for simplicity that $\omega_0$, $\omega_e$, $\omega_R^*$, $\mathscr{P}_T$ and $h$ do not change, then (26) can be rewritten as

$$\beta_c = \frac{h_c(\beta = 0)(\omega_0 + \tfrac{1}{2}\omega_e)}{h(\omega_0 + \omega_e)}. \quad (27)$$

That is, if $h_c$ is the cloud thickness in a well-mixed boundary layer, then if the layer becomes less well mixed the cloud will disappear for some value of $\beta_c \approx h_c/h$ since typically $\omega_e < \omega_0$. The first example in Table 1 gives a mixed layer cloud thickness of 49 mb, but this cloud layer disappears for $\beta_c = 0.33$.

It is clear that if the boundary layer is not well-mixed, it will be more difficult to maintain saturation below its top, and hence a solid cloud layer. Stratocumulus layers are rarely well mixed and hence (25) shows that the prediction of cloud layer thickness requires a realistic estimate of $\beta$. Boers and Betts (1988) found $\beta \approx 0.4$ within a time dependent stratocumulus layer off the West Coast of the USA. The second example in Table 1, with weaker subsidence and a deeper boundary layer, would have a thick cloud layer if well mixed, but over most of the oceans the cloud-top entrainment instability criterion (Randall, 1980; Deardorff, 1980) is met and the CBL is not well mixed. Typically we observe $\beta \approx 0.1$ to 0.2 in the subcloud layer and $\beta \approx 1$ in the cloud layer with a field of scattered cumulus clouds. Table 1 shows that layer cloud disappears in this diagnostic model for a layer mean value of $\beta > 0.6$. Formulae analogous to (25) become increasingly complicated for more complex CBL structures, and of course the assumption of horizontal homogeneity fails as the breakup of a cloud layer is reached.

### 3.3. *Diagnostic use of cloud thickness relationship*

Eq. (17) can be used diagnostically to estimate $\pi_0$ and $\pi_R$ for a well-mixed cloudy boundary layer in equilibrium. Fig. 2 shows an example. We observe a cloud-base at $\underset{\sim}{E}$. $\underset{\sim}{E}'$, found by going along a line of constant $q$ to the mixing line between $\underset{\sim}{O}$ and $\underset{\sim}{T}$, is the equilibrium state without radiative cooling. The radiative change of cloud thickness between $\underset{\sim}{E}'$ and $\underset{\sim}{E}$ is $h_R$:

$$h_R = \omega_R^* \tau = \pi_R h/(\pi_0 + h). \quad (28)$$

Substituting in (17) and rearranging gives the result

$$\pi_0 = h(h_c - h_R - \mathscr{P}_T)/(h - h_c + h_R). \quad (29)$$

This also follows directly from Fig. 2, since $\underset{\sim}{E}'$ is a weighted average of $\underset{\sim}{O}$ and $\underset{\sim}{T}$ in the ratio $\omega_0/\omega_e$ or $\pi_0/h$. Thus we can find $\pi_0$ and $\pi_R$ from (29) and (28) from observed values of $h$, $h_c$, $h_R$, and $\mathscr{P}_T$. Given $\omega_0$ (related to drag coefficient times surface wind) we have the divergence $D$, the entrainment and subsidence rate, $\omega_e$, and from $\omega_R^* = D\pi_R$, the mean radiative cooling rate of the boundary layer.

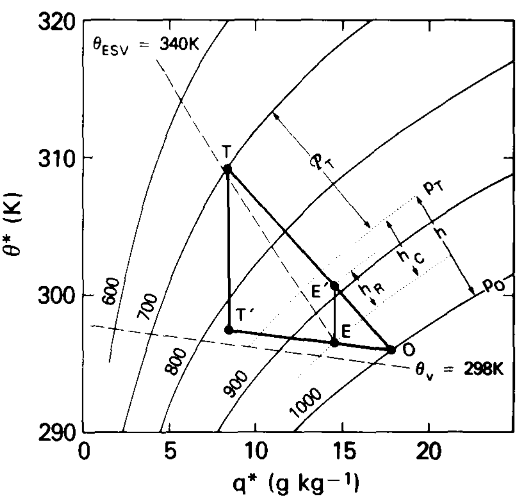


*Fig. 2.* As Fig. 1 for equilibrium mixed layer with net radiative cooling at cloud-top, showing diagnostic use of cloud thickness relationships. The dashed lines indicate the dry ($\theta_v$) and moist ($\theta_{ESV}$) virtual adiabats.

For partially mixed layers $\beta$ can be estimated and (25) used. The biggest practical limitation of this approach is the equilibrium assumption. Schubert et al. (1979a) showed that the mean boundary layer thermodynamic parameters adjust with the time-scale $\tau$ in (10), but the adjustment time for the boundary layer depth is determined by $h/\omega_e = D$, which is typically longer than $\tau$. Thus on timescales $\approx \tau$, a boundary layer may be close to internal thermodynamic equilibrium, but not have reached its equilibrium depth. In this case an analysis for a given depth $h$ will be correct in terms of the entrainment rate and radiative cooling; although entrainment and subsidence will not be in balance. This is equivalent in defining $\pi_0$, $\pi_R$ using an effective divergence $D'$ given by

$$\omega_e = D'h = Dh + \dot{h}.$$

The diagnostic analysis will give $\pi_0$, $\pi_R$; $D'$ and $\omega_e$ (from $\omega_0$), but the large scale subsidence cannot be separated from $\dot{h}$.

Fig. 2 illustrates the $p^*$ budget approximation (see Subsection 3.2 and Appendix). For example, $\underset{\sim}{E}'$ is defined most accurately as a weighted average of $\underset{\sim}{Q}$ and $\underset{\sim}{T}$ using $\theta^*$ and $q^*$. Using eq. (29), however, involves the neglect of the variations in the spacing of the isobars along $\underset{\sim}{Q}\underset{\sim}{E}'\underset{\sim}{T}$. Eq. (28) is a satisfactory method of finding $\pi_R$ since the pressure difference between $\underset{\sim}{E}'$ and $\underset{\sim}{E}$ is typically small. To the extent that we can neglect the changes in spacing and curvature of the isobars between $\underset{\sim}{T}\underset{\sim}{T}'$ and $\underset{\sim}{E}'\underset{\sim}{E}$ then $\pi_R$ is also just the pressure difference between $\underset{\sim}{T}$ and $\underset{\sim}{T}'$ (Betts, 1983).

Two other features of Fig. 2 are merely illustrative. $\underset{\sim}{Q}\underset{\sim}{E}$ has been drawn parallel to a dry virtual adiabat (constant virtual potential temperature, $\theta_v$) since a near-neutral subcloud layer is the typical equilibrium state over the ocean. $\underset{\sim}{T}\underset{\sim}{E}$ has been drawn slightly stable to the moist virtual adiabat which is the stability criteria for no cloud-top entrainment instability (Randall, 1980; Deardorff, 1980; Betts, 1983).

## 4. Evaporation of layer cloud by cloud-top mixing

Hanson (1984), Randall (1984), and Albrecht et al. (1985) have discussed how the thermodynamic properties of air entrained at cloud-top affects the rate of dissipation of a cloud layer. The results of Randall (1984) for a well mixed boundary layer are particularly simple (although approximate) when cast in the $p^*$ coordinate system.

The effect of cloud-top entrainment into a well-mixed layer can be isolated by neglecting the surface and radiative fluxes and the subsidence in eq. (3) giving (Randall, 1984)

$$h\dot{\underset{\sim}{M}} = \dot{h}(\underset{\sim}{T} - \underset{\sim}{M}), \tag{30}$$

where the mixed-layer thickness $h = p_0 - p_T$, and we have assumed $p_0$ is constant. The corresponding approximate saturation level budget equation is

$$h\dot{p}_M^* = (p_M^* - p_T^*)\,\dot{p}_T. \tag{31}$$

$\dot{p}_M^*$, and $\dot{p}_T$ are respectively the rate of rise of cloud-base and cloud-top due to the entrainment process. The cloud thickness will deepen or get thinner as both base and top rise, according to whether

$$\frac{\dot{p}_T}{\dot{p}_M^*} = \left(\frac{h}{p_M^* - p_T^*}\right) \gtrless 1. \tag{32}$$

We can rewrite this condition as

$$\frac{h_c + h_{sc}}{h_c + |\mathscr{P}_T|} \gtrless 1, \tag{32'}$$

where $h_c$, $h_{sc}$ are the pressure thicknesses of the cloud and subcloud layers respectively. Thus, the condition for the cloud layer deepening or getting thinner can also be written as

$$h_{sc} \gtrless |\mathscr{P}_T|. \tag{33}$$

We see that if the subcloud layer (which is coupled to the cloud layer by the well-mixed layer assumption) is deeper than $\mathscr{P}_T$, the measure of the subsaturation of air entrained at cloud top, then the rise of cloud-base will be slower than the rate of deepening by entrainment, and the cloud-layer will get thicker as it rises. Thus, under some conditions (inequality (33): corresponding to sufficiently moist entrained air or a deep subcloud layer), cloud-top entrainment will not tend to dissipate cloud (Randall, 1984). The inequality (33) is dependent, however, on the mixed-layer assumption. Rapid cloud-top entrainment may well produce a layer that is not well mixed, and we have shown in Section 3 that in equilibrium, this will give a much thinner mean cloud layer.

The above analysis also shows that if the cloud layer itself stays well mixed but uncouples from the subcloud layer (Nicholls, 1984), then cloud-top entrainment will always tend to thin the cloud layer. The mixed layer thickness becomes $h_c$ in (31), and (32) becomes

$$\frac{\dot{p}_T}{\dot{p}_M^*} = \frac{h_c}{h_c + |\mathscr{P}_T|} < 1. \tag{34}$$

## 5. Conclusions

We have shown how an idealized model using the saturation pressure budget approximation gives the equilibrium cloud depth for well-mixed boundary layers as a sum of the forcing processes: the surface transfer, the entrainment of dry air at the CBL top and the bulk radiative cooling. The effect on cloud thickness of the surface fluxes (through the surface wind and bulk transfer coefficient), and the mean divergence of the horizontal wind appear only combined in a surface transfer pressure scale, $\pi_0$. The bulk radiative cooling of the CBL can be expressed as a presssure scale $\pi_R$. These solutions show that an equilibrium well mixed layer will always be cloudy unless there is strong low level divergence because $\pi_0 + \pi_R > |\mathscr{P}_T|$, a measure of the subsaturation of the dry air sinking into the CBL. However, these solutions also show that the thickness of layer cloud in a boundary layer is very sensitive to the "well-mixed layer" assumption. Partially mixed layers will tend to have much thinner layer cloud.

These equilibrium relationships are primarily of diagnostic interest, since neither boundary layer depth nor entrainment rate have been predicted. They indicate the relative importance of different processes in determining cloud thickness, and can be used diagnostically to estimate mean divergence, entrainment rate, and radiative cooling in boundary layers near equilibrium from other parameters that are more easily observed, such as the surface wind, cloud and boundary layer depths, and the thermodynamic structure.

The analysis of cloud deepening by cloud-top entrainment of Randall (1984) has been expressed using the $p^*$ budget approximation. This shows that the criterion for cloud-top deepening by entrainment depends on the ratio of the depth of the subcloud layer to the saturation pressure departure (a measure in $p^*$ coordinates of the subsaturation) of the air entrained at cloud-top. Cloud layers that uncouple from the surface will always thin by cloud-top mixing.

## 6. Acknowledgements

This research has been supported by the Global Atmospheric Research Program of the National Science Foundation under grant ATM87-05403 and the National Aeronautics and Space Administration under contract NAS5-28800, through the Goddard Space Flight Center.

## 7. Appendix

*Saturation pressure budget approximation*

The total water ($q^*$) budget is accurate in the absence of precipitation. The saturation (or liquid water) potential temperature budget is reasonably accurate. Uncertainties (of order a few percent) exist, associated with the generation and dissipation of kinetic energy (Betts, 1974a), and if these are neglected, a layer mean value of $(T/\theta)$ can be used to convert between the mean $T$ and $\theta$ budgets for a CBL. In addition horizontal variations of $\theta^*/\theta$ must be neglected in mixing processes, but these are typically small ($\approx 1\%$) in layer clouds. The saturation pressure budget involves a larger approximation, which becomes clearer if we express variations of $p^*$ as a linear combination of $\theta^*$ and $q^*$

$$\delta p^* = a\,\delta\theta^* + b\,\delta q^*, \tag{A1}$$

where

$$a = (\partial p^*/\partial\theta^*)_{q^*}, \quad b = (\partial p^*/\partial q^*)_{\theta^*}.$$

To the extent that we can neglect the variations of the gradients $a$ and $b$ in a shallow layer, then the $p^*$ budget is as accurate as the $\theta^*$, and $q^*$ budgets.

However, if we consider the budget equation

$$0 = \omega_0(\underset{\sim}{Q} - \underset{\sim}{E}) + \omega_c(\underset{\sim}{T} - \underset{\sim}{E}), \tag{A2}$$

we find that $a$ and $b$ in (A1) can vary by as much as 20% between the extreme SP's of the surface and that of the entrained air $\underset{\sim}{T}$, so that computing

Table 2. *Non-linearity of $p^*$ on mixing line*

| $\theta^*$ (K) | $q^*$ ($g$ kg$^{-1}$) | $p^*$ (mb) | $\Delta p^*$ (mb) |
|---|---|---|---|
| 298 | 17 | 960.5 | |
| 300 | 15 | 906.4 | 54.1 |
| 302 | 13 | 852.3 | 54.1 |
| 304 | 11 | 797.7 | 54.7 |
| 306 | 9 | 741.7 | 56.0 |
| 308 | 7 | 682.9 | 58.8 |
| 310 | 5 | 618.5 | 64.4 |

$p_E^*$ from

$$0 = \omega_0(p_0^* - p_E^*) + \omega_e(p_T^* - p_E^*), \tag{A3}$$

rather than from $\theta_E^*$, $q_E^*$ found from the corresponding $\theta^*$, and $q^*$ equations, can give an error in $p_E^*$ as large as 10 mb. Nonetheless, the approximation implied by the linearization (A1) is qualitatively useful to understand the controls of stratocumulus layer depth discussed in this paper.

Another way of visualizing this approximation is to consider the non-linearity of $p^*$ on a mixing line: a line of constant $d\theta^*/dq^*$. Table 2 shows a typical tropical CBL mixing line and the change $\Delta p^*$ for equal increments of $\Delta\theta^* = \Delta q^* = 1$. For saturation levels within the CBL (say 960–800 mb), the non-linearity of $\Delta p^*$ is small ($\approx 1\%$). It is only large for the much drier SP's typical of the entrained air. From an observational viewpoint, the error introduced by this approximation is equivalent (for the data here) to introducing an error in $q$ of the entrained air of 0.7 $g$ kg$^{-1}$, which is comparable to typical measurement or sampling errors.

## REFERENCES


Albrecht, B. A. 1979. A model of the thermodynamic structure of the trade-wind boundary layer: Part II. Applications. *J. Atmos. Sci. 36*, 90–98.

Albrecht, B. A. 1981. Parameterization of trade-cumulus cloud amounts. *J. Atmos. Sci. 38*, 97–105.

Albrecht, B. A., Betts, A. K., Schubert, W. H. and Cox, S. K. 1979. A model of the thermodynamic structure of the trade-wind boundary layer: Part I. Theoretical formulation and sensitivity tests. *J. Atmos. Sci. 36*, 73–89.

Albrecht, B. A., Penc, R. and Schubert, W. 1985. An observational study of cloud-topped mixed layers. *J. Atmos. Sci. 42*, 800–822.

Augstein, E. and Wendel, M. 1980. Modelling of the time-dependent atmospheric trade-wind boundary layer with non-precipitating cumulus clouds. *Beitr. Phys. Atmos. 53*, 509–538.

Betts, A. K. 1973. Non-precipitating cumulus convection and its parameterization. *Quart. J. Roy. Met. Soc. 99*, 178–196.

Betts, A. K. 1974a. Further comments on "A comparison of the equivalent potential temperature and the static energy". *J. Atmos. Sci. 31*, 1713–1715.

Betts, A. K. 1974b. Reply to comment on the paper "Non-precipitating cumulus convection and its parameterization". *Quart. J. Roy. Meteor. Soc. 100*, 469–471.

Betts, A. K. 1975. Parametric interpretation of trade-wind cumulus budget studies. *J. Atmos. Sci. 32*, 1934–1945.

Betts, A. K. 1976. Modelling subcloud layer structure and interaction with a shallow cumulus layer. *J. Atmos. Sci. 33*, 2363–2382.

Betts, A. K. 1982. Saturation point analysis of moist convective overturning. *J. Atmos. Sci. 39*, 1484–1505.

Betts, A. K. 1983. Thermodynamics of mixed stratocumulus layers: saturation point budgets. *J. Atmos. Sci. 40*, 2655–2670.

Betts, A. K. 1986. A new convective adjustment scheme. Part I: Observational and theoretical basis. *Quart. J. Roy. Meteor. Soc. 112*, 677–691.

Betts, A. K. and Albrecht, B. A. 1987. Conserved variable analysis of boundary layer thermodynamic structure over the tropical oceans. *J. Atmos. Sci. 44*, 83–99.

Betts, A. K. and Ridgway, W. 1988. Coupling of the radiative, convective and surface fluxes over the equatorial Pacific. *J. Atmos. Sci. 45*, 522–536.

Boers, R. and Betts, A. K. 1988. Saturation point structure of marine stratocumulus clouds. *J. Atmos. Sci. 45*, 1156–1175.

Deardorff, J. W. 1980. Cloud-top entrainment instability. *J. Atmos. Sci. 37*, 131–147.

Deardorff, J. W., Willis, G. E. and Lilly, D. K. 1974. Comment on the paper by A. K. Betts. "Non-precipitating cumulus convection and its parameterization". *Quart. J. Roy. Meteor. Soc. 100*, 122–123.

Fitzjarrald, D. R. 1982. New applications of a simple mixed layer model. *Bound. Layer Meteor. 22*, 431–451.

Hanson, H. 1984. On mixed layer modelling of the stratocumulus topped marine boundary layer. *J. Atmos. Sci. 41*, 1226–1236.

Lilly, D. K. 1968. Models of cloud-topped mixed layers under a strong inversion. *Quart. J. Roy. Meteor. Soc. 94*, 292–309.

Nicholls, S. 1984. The dynamics of stratocumulus: Aircraft observations and comparisons with a mixed layer model. *Quart. J. Roy. Meteor. Soc. 110*, 783–820.

Ogura, Y. and Cho, H.-R. 1974. On the interaction between the subcloud and cloud layers in tropical regions. *J. Atmos. Sci. 31*, 1850–1859.

Randall, D. A. 1980. Conditional instability of the first kind upside-down. *J. Atmos. Sci. 37*, 125–130.

Randall, D. A. 1984. Stratocumulus cloud deepening through entrainment. *Tellus 36A*, 446–457.

Sarachik, E. S. 1974. The tropical mixed layer and cumulus parameterization. *J. Atmos. Sci. 31*, 2225–2230.

Schubert, W. H. 1976. Experiments with Lilly's cloud-topped mixed layer model. *J. Atmos. Sci. 33*, 436–446.

Schubert, W. H., Wakefield, J. S., Steiner, E. J. and Cox, S. K. 1979a. Marine stratocumulus convection. Part I: Governing equations and horizontally homogeneous solutions. *J. Atmos. Sci. 36*, 1286–1307.

Schubert, W. H., Wakefield, J. S., Steiner, E. J. and Cox, S. K. 1979b. Marine stratocumulus convection. Part II: Horizontally inhomogeneous solutions. *J. Atmos. Sci. 36*, 1308–1324.

Stage, S. A. and Businger, J. A. 1981a. A model for entrainment into a cloud-topped boundary layer. Part I: Model description and application to a cold air outbreak. *J. Atmos. Sci. 38*, 2213–2229.

Stage, S. A. and Businger, J. A. 1981b. A model for entrainment into a cloud-topped boundary layer. Part II: Discussion of model behavior and comparison with other models. *J. Atmos. Sci. 38*, 2230–2242.